Binuclear oxalamidinate complexes (MePd)₂(oxam) and homoleptic complexes of the type [(THF)$_n$Li₄(Me₈)M₂] and [(THF)₄Li₂(Ph₄)M] (M = Pd, Ni): synthesis, structures and catalytic C–C linking reactions

Katja Lamm, Michael Stollenz, Mirko Meier, Helmar Görls, Dirk Walther *

Institut für Anorganische und Analytische Chemie der Friedrich-Schiller-Universität Jena, August-Bebel-Straße 2, D-07743 Jena, Germany

Abstract

The dinuclear methyl complexes **1** and **2** of the type [CH₃–Pd(oxam)Pd–CH₃] were obtained by reaction of (COD)PdCH₃(Cl) with the corresponding dilithium oxalic amidinates, prepared from LiBu and the oxalic amidines H₂Y or H₂Z (H₂Y = N,N'-bis(2-pyridylethyl)-1,2-bis-(2,4,6-trimethylphenyl-imino)-ethane-1,2-diamine; H₂Z = N,N'-bis(diphenylphosphino-3-propyl)-1,2-bis-(2,4,6-trimethylphenyl-imino)-ethane-1,2-diamine). Reaction of both **1** and **2** with an excess of LiCH₃ results in the formation of the dimeric compound [(THF)₄Li₄(CH₃)₈Pd₂] (**3**). Similarly, monomeric phenyl complexes of the composition [(THF)₄Li₂M(C₆H₅)₄] (M = Pd (**4**), Ni (**5**)) were prepared. The complexes were characterized by elemental analysis, mass spectroscopy, ¹H-NMR, ¹³C-NMR and ⁷Li-NMR spectroscopy, and by X-ray single-crystal diffraction analysis in the solid state. All complexes contain the metals in a planar-square environment. Compounds **1–3** and **4** are highly active, selective and long-living catalysts in the Heck reaction of 4-bromoacetophenone and *n*-butyl acrylate. Compound **5** and the related neutral ligand-free Ni complex [(THF)₄Li₄(CH₃)₈Ni₂] (**6**) are active catalysts for the Kumada cross-coupling of MesitylMgBr with 4-bromotoluene and are even able to couple the corresponding aryl chloride or aryl fluoride with MesitylMgBr.

1. Introduction

Homoleptic transition metal methyl complexes of the type [M(CH₃)$_n$] are only known for d-electron-poor metals in high oxidation states whereas such complexes of d-electron-rich transition metals with "normal" oxidation states are unstable. However, stable complexes with d-electron-rich metals can be obtained by occupying additional coordination positions around the metal by methyl groups resulting in the formation of dimeric compounds of the type [(solv)$_n$Li₄(CH₃)₈M(II)₂] (**A**) (Scheme 1) [1–10]. Similarly, phenyl complexes of transition metals can be stabilized by the formation of monomeric complexes of the composition [(solv)$_n$-Li₂M(C₆H₅)₄] (**B**) (Scheme 1) [10,11].

The first methyl complex of the type **A** containing Cr(II) was isolated by Kurras and Otto [1] in the early 1960s. Recently, we have isolated and structurally determined two methyl Ni(II) complexes of the type **A** (*n* = 2 or 4) [8]. Independently, Ihara et al. [9] prepared the Ni complex with *n* = 4. Surprisingly, Pd complexes of the type **A** and **B** which would have been of particular interest in catalysis are still unknown.

Due to their high reactivity, complexes of the type **A** and **B** may act as starting material for the synthesis of other organometallics. However, surprisingly less is known about their potential as catalysts in homogeneous-catalytic reactions [9].

We report in this publication, the synthesis and structure of the new binuclear complex [(THF)₄Li₄(CH₃)₈Pd₂] (**3**) formed, for example, by reaction of the hitherto unknown

* Corresponding author. Tel.: +49-3641-948-119; fax: +49-3641-948-102.
E-mail address: cdw@rz.uni-jena.de (D. Walther).
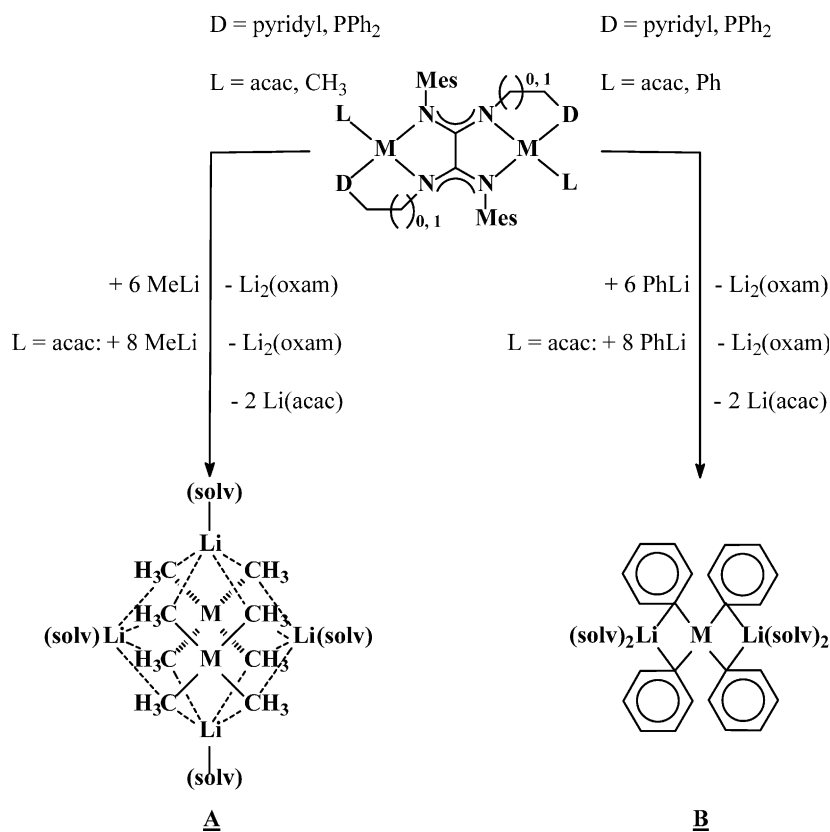
Scheme 1. Complex types **A** and **B**.

oxalic amidinate complexes **1** and **2** of the type [CH₃–Pd(oxam)Pd–CH₃] with an excess of LiCH₃ (oxam: three-dentate oxalic amidinates containing N- or P-donor atoms in the side chains). Furthermore, we describe the synthesis and structure of the complexes [(THF)$_4$Li$_2$M(C$_6$H$_5$)$_4$] (M = Pd (**4**), Ni (**5**)[11]). Additionally, we show that the Pd complexes **1**–**3** and **4** are extremely active catalysts in the Heck reaction, whereas (THF)$_4$Li$_2$NiPh$_4$ and [(THF)$_4$Li$_4$(CH$_3$)$_8$Ni(II)$_2$] (**6**) are catalytically active in the Kumada C–C coupling even if an aryl chloride or an aryl fluoride were used as coupling components. It is somewhat surprising that the complexes **3**–**6** are active, long-living catalysts in these reactions, since the generally accepted mechanisms of both catalytic cycles contain the redox steps M(II)/M(0) and M(0)/M(II) which usually require additional neutral π-acceptor ligands for stabilizing the low oxidation state of the metal in solution. The complexes **3**–**6**, however, do not contain such stabilizing ligands.

2. Results

2.1. Synthesis and structures of the methyl palladium complexes 1–3

The reaction of (COD)PdCH₃(Cl) with two equivalents of Li$_2$Y (H$_2$Y = N^1,N^2-bis(2-pyridylethyl)-N^3,N^4-

bis(2,4,6-trimethylphenyl)-oxalamidinate) [12,13] in THF at −78 °C resulted in the formation of a yellow solution from which the pure dinuclear methyl palladium(II) compound **1** could be isolated in 55% yield (Scheme 2). Single crystals of **1** were grown from THF.

Similarly, complex **2**, containing two phosphorous donor atoms in the side arms, could be synthesized using Li$_2$Z (Scheme 2). Both complexes are readily soluble in toluene or THF and are thermally stable even for several hours in toluene solution at 100 °C. Elemental analysis and mass spectrum confirmed their composition.

In the mass spectrum of **1**, the binuclear complex ion [CH₃Pd(oxam)Pd]⁺ (m/z = 757) was detected. The ¹H-NMR spectrum of **1** at ambient temperature in THF-d_8 is very similar to that of the corresponding Ni methyl complex [8] with one singlet of the methyl protons of the Pd–Me group at $\delta = -0.55$ ppm and two singlets for the methyl mesityl groups at $\delta = 2.29$ ppm (p-methyl) and 2.18 ppm (o-methyl). The relative intensities of these resonances were 1:1:2. In addition to the signals corresponding to the protons of the aromatic rings between 6.65 and 8.35 ppm, the ¹H-NMR spectrum showed two broad singlets at 2.26 and 2.86 ppm, which are assigned to the CH₂ groups.

The ¹³C-NMR spectrum in THF-d_8 also showed a very simple pattern. The resonance for the carbon of the Pd–CH₃ groups was found at $\delta = 4.9$ ppm, and the
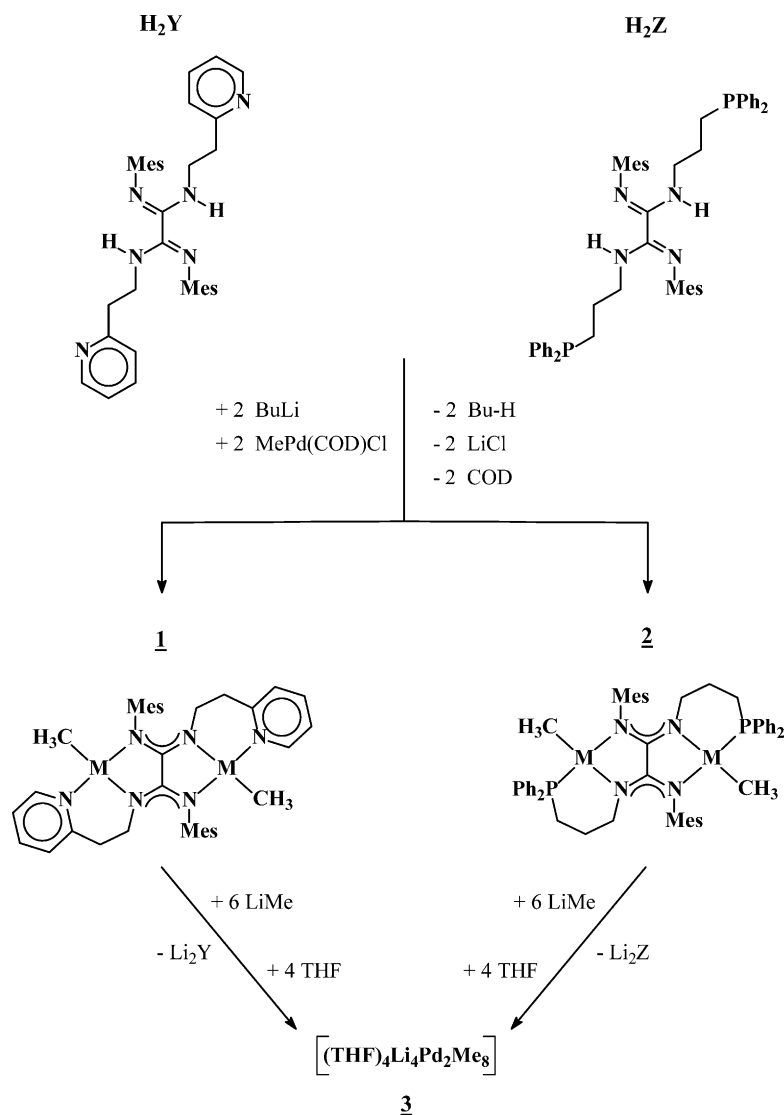
Scheme 2. Synthesis of the complexes **1**–**3**.

signals of the mesityl–Me carbons appeared at 19.4 and 21.0 ppm, respectively. Furthermore, the resonances for the CH$_2$ carbons were observed at 43.4 and 44.6 ppm. In addition, only nine resonances in the region of the sp^2-carbons between 123.1 and 167.3 ppm were observed. This is typical for a symmetrical structure in solution and corresponds to five signals for the inequivalent aromatic CH groups, one signal at 167.3 ppm for the equivalent oxalamidinate carbons and four signals for the inequivalent quarternary C atoms of the aromatic substituents. The expected number of the latter signals was 5; possibly, one signal may be too weak or does overlap with other signals in this region.

The solid-state structure of **1** determined by an X-ray analysis is shown in Fig. 1. Relevant bond lengths and angles are listed in the figure caption. The dinuclear complex contains two Pd(II) centers connected via the oxam ligand Y which acts in a bis-chelating tridentate

fashion. Each metal ion is in a planar environment created by three N atoms from the chelating ligand and one carbon of the methyl group. The C1–C2 bond distance in the chelating ligand (1.526(7) Å) is that of a single bond. Furthermore, bond angles around both carbons are typical for sp^2-hybridization. As expected, the two methyl groups coordinated to the Pd centers of the oxam bridge lie *trans* to each other. The Pd–C bonds (2.025(5) Å) fall in a typical range. The solid-state structure of **2**, shown in Fig. 2, is similar to that of **1**. The coordination environment of the Pd atoms is also nearly planar (deviation 0.0356 Å) and the C–N bonds of the oxalamidinate bridge are almost equivalent, indicating a high double-bond character due to a complete electron delocalization over the two NCN units (1.317(3) Å; C1–N2, 1.338(3) Å).

NMR studies in THF-d_8 confirm that **2** has a similar structure in solution as in the solid state. In the ^{1}H-
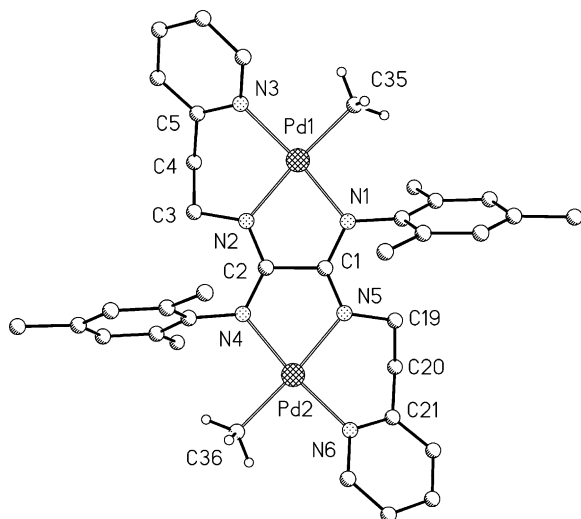
Fig. 1. Molecular structure of complex **1**.

NMR spectrum, the proton signals for the mesityl methyl groups are observed at $\delta = 2.15$ and 2.31 ppm, and the methylene protons give three broadened signals in the ranges 1.44–1.51, 1.84–1.90 and 2.59–2.61 ppm. Additionally, a doublet for the methyl–Pd protons at $\delta = -0.85$ ppm was found.

Selected bond distances (Å) and bond angles (°): Pd1–N1, 2.029(4)°; Pd1–N2, 2.068(4)°; Pd1–N3, 2.061(4)°; Pd1–C35, 2.025(5)°; Pd2–N4, 2.043(3)°; Pd2–N5, 2.086(4)°; Pd2–N6, 2.057(4)°; C1–N1, 1.342(6)°; C1–C2, 1.526(7)°; C1–N5, 1.291(6)°; C2–N2, 1.312(6)°; C2–N4, 1.337(6)°; N2–C3, 1.463(7)°; C3–C4, 1.544(7)°; C4–C5, 1.504(8)°; C5–N3, 1.350(7)°; N5–C19, 1.447(6)°; C19–C20, 1.539(7)°; C20–C21, 1.495(8)°; C21–N6, 1.373(7)°; C35–Pd1–N1, 95.1(2) Å; C35–Pd1–N2, 174.3(2) Å; C35–Pd1–N3, 91.2(2) Å; N1–Pd1–N2, 79.7(2) Å; N1–Pd1–N3, 173.7(2) Å; N2–Pd1–N3, 94.0(2) Å; C36–Pd2–N4, 95.2(2) Å; C36–

Fig. 2. Molecular structure of complex **2**.

Pd2–N5, 174.2(2) Å; C36–Pd2–N6, 91.2(2) Å; N4–Pd2–N5, 79.6(2) Å; N4–Pd2–N6, 173.6(2) Å; N5–Pd2–N6, 94.0(2) Å; N1–C1–N5, 131.0(5) Å; N2–C2–N4, 130.6(5) Å.

Selected bond distances (Å) and bond angles (°): Pd–C26, 2.077(2)°; Pd–P1, 2.2077(6)°; Pd–N1, 2.092(2)°; Pd–N2A, 2.081(2)°; C1–N1, 1.317(3)°; C1–N2, 1.338(3)°; N1–C2, 1.468(3)°; C2–C3, 1.525(3)°; C3–C4, 1.543(3)°; C4–P1, 1.821(2)°; C26–Pd–P1, 86.48(6) Å; C26–Pd–N1, 172.90(8) Å; C26–Pd–N2A, 95.66(8) Å; P1–Pd–N1, 99.68(5) Å; P1–Pd–N2A, 172.15(5) Å; N1–Pd–N2A, 78.70(7) Å; N1–C1–N2, 131.0(2) Å; N1–C1–C1A, 115.2(2) Å; N2–C1–C1A, 113.8(2) Å.

Symmetry transformations used to generated equivalent atoms: A $-X$, Y, $-Z-1/2$.

For the synthesis of the cluster complex **3**, three routes starting either from **1**, **2** or from dinuclear complexes of the type [(acac)Pd(oxam)Pd(acac)] [14] could be used. Reaction of **1** or **2** with six equivalents of LiMe in THF at $-78\,^\circ$C resulted in a yellow solution from which **3** could be isolated in 20% yield (Scheme 2). Furthermore, [(acac)Pd(oxam)Pd(acac)] reacted with eight equivalents of LiMe in THF at $-78\,^\circ$C to form a brown suspension which turned to a yellow solution by slowly warming to room temperature. Upon evaporation of most of the solvent and keeping the resulting solution at $-25\,^\circ$C, colorless crystals of **3** could be isolated in 20% yield. The pyrophoric complex is extremely sensitive towards traces of air or moisture. It is soluble in THF, toluene and benzene.

Its ^{1}H-NMR spectrum (in C_6D_6 at room temperature) showed only one singlet at -0.11 ppm besides the proton resonances of the coordinated THF at 1.30 and 3.72 ppm indicating that the methyl groups are equivalent. The symmetrical structure of the complex was confirmed by the ^{13}C-NMR spectrum showing only one signal for the methyl group at -7.6 ppm, and by the ^{7}Li-NMR spectrum in which also only one signal at 9.3 ppm was observed.

Single crystals of **3** were obtained from THF suitable for X-ray crystallographic determination. The crystal structure confirmed the highly symmetrical structure in solution indicated by NMR spectroscopy. Fig. 3 displays the dimeric molecular structure and selected bond lengths and angles in the figure caption. The structure is very similar to the corresponding dimeric Ni(II) compound [8]. Each palladium ion in **3** is surrounded by four methyl groups in a square-planar geometry. The eight methyl groups of the dimer are situated at the corners of a cube. The Pd centers are placed in the middle of two squares lying on opposite sides. The Pd$\cdots$Pd separation is relatively long (3.279(2) Å) confirming the absence of a metal–metal bond between those two metal centers. In the middle of the other four squares of the Me$_8$ cube, the four Li ions are situated. Each Li atom coordinates one THF molecule and
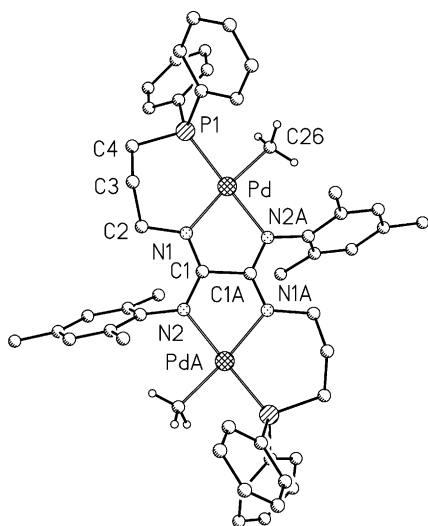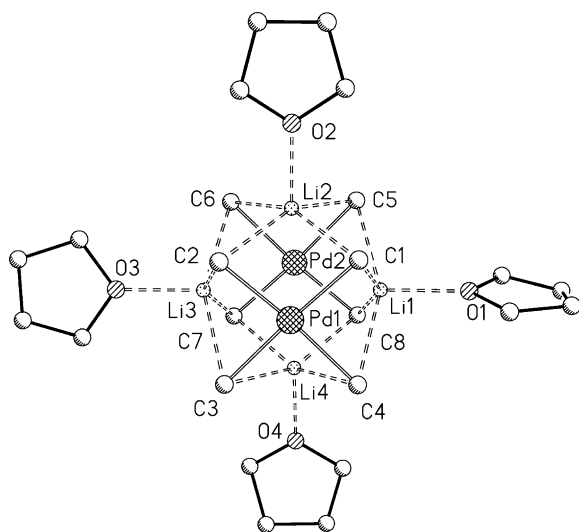
Fig. 3. Molecular structure of complex **3**.

interacts with the carbon atoms of four methyl groups forming Pd–CH$_3$–Li bonds. The C–Li(THF) distances (average 2.431 Å) fall in a typical range. The Pd–CH$_3$ distances range from 2.120 to 2.143 Å (average 2.135 Å), which is slightly larger than the respective bond distances in comparable square-planar dimethyl–Pd complexes that consist of additional P,P, P,N or N,N chelating ligands. Their Pd–CH$_3$ bond distances are ranged from 2.016 to 2.097 Å.

Selected bond distances (Å) and bond angles (°): Pd1–C1, 2.142(3)°; Pd1–C2, 2.134(3)°; Pd1–C3, 2.120(3)°; Pd1–C4, 2.139(3)°; Pd2–C5, 2.137(3)°; Pd2–C6, 2.126(3)°; Pd2–C7, 2.143(3)°; Pd2–C8, 2.137(3)°; Li1–C1, 2.426(7)°; Li1–C4, 2.419(6)°; Li1–C5, 2.441(6)°; Li1–C8, 2.440(7)°; Li1–O1, 2.036(6)°; Li2–C1, 2.396(7)°; Li2–C2, 2.442(7)°; Li2–C5, 2.433(7)°; Li2–C6, 2.444(7)°; Li2–O2, 2.006(6)°; Li3–C2, 2.435(7)°; Li3–C3, 2.432(7)°; Li3–C6, 2.428(7)°; Li3–C7, 2.447(7)°; Li3–O3, 2.032(6)°; Li4–C3, 2.464(7)°; Li4–C4, 2.407(7)°; Li4–C7, 2.416(7)°; Li4–C8, 2.426(7)°; Li4–O4, 2.000(6)°; C1–Pd1–C2, 89.7(1) Å; C1–Pd1–C3, 169.4(1) Å; C1–Pd2–C4, 90.5(1) Å; C5–Pd2–C6, 88.7(1) Å; C5–Pd2–C7, 169.5(1) Å; C5–Pd2–C8, 89.6(1) Å.

According to these results, the solid-state structure of **3** is very similar to those of the corresponding Cr(II), Mo(II) and Ni(II) compounds. The only remarkable difference to the Cr(II) complex is the very large Pd···Pd separation found in **3**, in contrast to the very short Cr···Cr distance (1.968(2) Å) in the corresponding Cr complex [1]. It is, however, in agreement with the large M···M separations in the corresponding Ni and Pt complexes [7,8]. In other words, a short M···M contact is no prerequisite for the stabilization of cluster complexes of the type [M$_2$(CH$_3$)$_8$]$^{n-}$.

2.2. Phenyl complexes (THF)$_4$Li$_2$PdPh$_4$ (**4**) and (THF)$_4$Li$_2$NiPh$_4$ (**5**)

The so far unknown complex (THF)$_4$Li$_2$PdPh$_4$ (**4**) was synthesized starting with the dinuclear complex [(acac)Pd(oxam)Pd(acac)] in a THF solution and eight equivalents of Li(C$_6$H$_5$) at −78 °C (Scheme 3). After concentrating the brown reaction mixture, colorless crystals could be grown at −25 °C. Like the above-described homoleptic compound **3**, they show an extreme sensitivity towards air and moisture and a comparable solubility. Therefore, only Li and Pd content could be determined by ICP-MS supporting the above composition.

The ^{1}H-NMR spectrum in C$_6$D$_6$ shows two singlets for the CH$_2$ groups of the coordinated THF molecules at 1.38 and 3.51 ppm. The aromatic CH protons of the phenyl groups give a doublet at 8.16 and three multiplets at 6.95–6.99, 7.11–7.22 and 7.44–7.47 ppm which cannot be integrated because of the overlapping with the solvent signal. In the ^{13}C-NMR spectrum, two signals for the THF molecules at 25.9 and 68.0 ppm appear, the signals for the phenyl groups are once more difficult to separate from the solvent signals. At least two signals can be found at 122.2 and 141.2 ppm. The ^{7}Li-NMR spectrum shows only one signal at 7.1 ppm, which supports the highly symmetrical structure of compound **4**.

Fig. 4 displays the molecular structure and selected bond lengths and angles in the figure caption for the Pd complex **4** in the solid state determined by X-ray analysis of single crystals.

Selected bond distances (Å) and bond angles (°): Pd–C1, 2.095(5)°; Pd–C7, 2.102(5)°; Pd–C13, 2.090(5)°; Pd–C19, 2.091(5)°; Li1–C1, 2.348(10)°; Li1–C7, 2.275(9)°; Li1–O1, 1.928(9)°; Li1–O2, 1.930(9)°; Li2–C13, 2.368(9)°; Li2–C19, 2.258(9)°; Li2–O3, 1.975(9)°; Li2–O4, 1.960(9)°; C1–Pd–C7, 95.4(2) Å; C1–Pd–C13, 84.5(2) Å; C1–Pd–C19, 178.8(2) Å; C7–Pd–C13, 178.5(2) Å; C7–Pd–C19, 85.5(2) Å; C13–Pd–C19, 94.7(2) Å.

Each Pd center is surrounded by four σ-bounded phenyl groups in a square-planar geometry. Furthermore, two Li ions are bound on opposite sides of the PdC$_4$ square, each forming two Li–C–Pd bridges with the *ipso*-carbons of the phenyl groups. Additionally, each Li coordinates two THF molecules in a distorted tetrahedral geometry. The C–Pd–C angles at the Li-coordinated side (average 95°) are slightly larger than the C–Pd–C angles where no Li ion is placed (average 85°). The Li–C distances are in the range of typical covalent bondings and the Pd–C distances (average 2.095 Å) fall also in the typical range. The phenyl groups are distorted out of the plane of the *ipso*-carbon atoms and are oriented towards the respective Li atom.
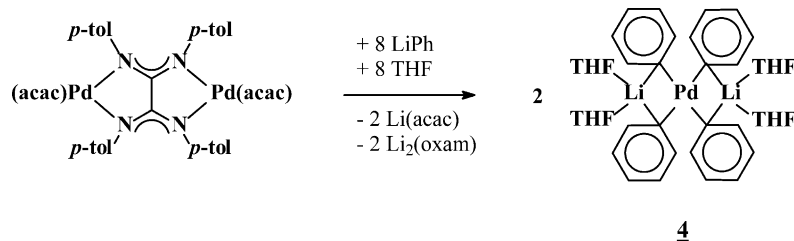
Scheme 3. Formation reaction of the Pd complex **4**.
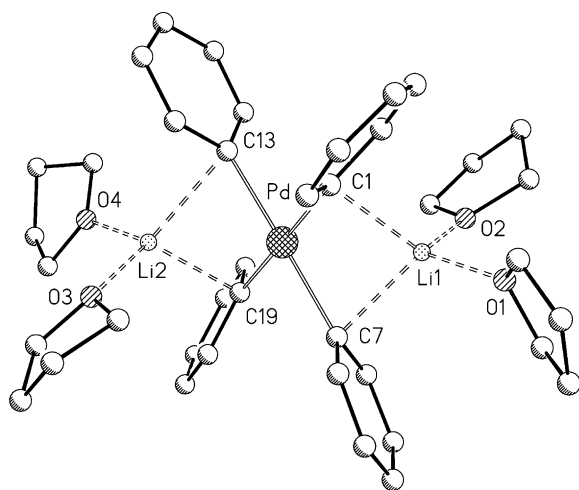
Fig. 4. Molecular structure of complex **4**.

Our synthetic route to obtain the corresponding Ni complex **5**, first prepared by Taube and Honymus [10], was similar to that of the preparation of the methyl complex $(THF)_4Li_4Ni_2Me_8$. Starting with the complex [(acac)Ni(oxam)Ni(acac)] [14], the addition of eight equivalents of $Li(C_6H_5)$ at $-78\,^{\circ}C$ in a THF solution results in a dark brown solution by warming slowly to room temperature. Complex $(THF)_4Li_2NiPh_4$ (**5**) can then be isolated by evaporating most of the solvent and cooling the THF residue to $-25\,^{\circ}C$ for 3 days. Yellow crystals form, which are sensitive towards air and moisture. The complex is soluble in THF, toluene and benzene.

Its ^1H-NMR spectrum (in C_6D_6 at room temperature) shows two singlets for the CH_2 groups of the coordi-

overlapped by the signal for the solvent C_6D_6. This does not allow an exact integration for determining the ratio of bound phenyl groups to coordinated THF molecules. However, Ni and Li analyses using ICP-MS analysis suggested the composition to be $(THF)_4Li_2NiPh_4$.

The ^7Li-NMR spectrum displays only one signal for the two Li atoms at 6.5 ppm which is in agreement with a symmetrical structure in solution. The X-ray diffraction analysis of single crystals confirmed this structure in the solid state. The molecular structure of the Ni complex **5** (not depicted) is very similar to that of the corresponding Pd complex **4** (Fig. 4) and need therefore no further discussion.

2.3. Catalytic Heck reaction with **1–4**

The Heck coupling is known to be a very useful catalytic C–C linking reaction for the formation of substituted arylated olefins starting from Ar–X and substituted olefins [15–18]. This reaction is catalyzed by a variety of palladium complexes with different controlling ligands. Palladacycles with C, P coordination [19–21] and carbene palladium complexes [22–25] belong to the most active catalysts. Furthermore, various phosphines and phosphites are powerful ligands for the activation of aryl chlorides [26,27].

To test the ability of **1**, **2**, **3** and **4** in catalyzing the Heck reaction and to compare their catalytic activities, we used in initial catalytic experiments the substrates 4-bromoacetophenone and *n*-butyl acrylate which were reacted in dimethylacetamide as solvent to give (*E*)-4-acetylcinnamate as cross-coupling product (Eq. (1)):

(1)
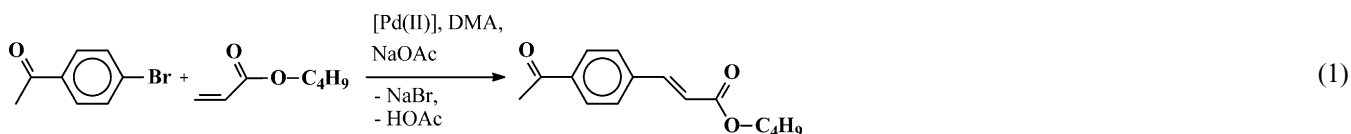
nated THF molecules at 1.36 and 3.41 ppm. For the phenyl groups, various multiplets between 6.84 and 7.18, 7.46 and 7.50, and 8.28 and 8.31 ppm show, which are

Table 1 contains selected results which show that all four complexes are highly active catalysts when the catalyses were carried out in the presence of sodium

Table 1
Heck reaction catalyzed by the Pd complexes **1**–**4**

Entry	Catalyst	Temperature (°C)	Complex (mol%)	Time (h)	Conversion (%)	Selectivity (%)	TON [a]	TOF [b]
1	1	120	0.02	10	98	83	4900	490
2	2	120	0.02	10	98	81	4900	490
3	3	120	0.02	1	>99	94	5000	5000
4	3	100	0.02	1.5	90	98	4500	2900
5	3	120	0.0002	15	87	100	435000	29000
6	4	120	0.04	1	98	91	2450	2450

Conditions: 6.25 mmol = one equivalent of 4-bromoacetophenone, 1.08 equivalents of *n*-butyl acrylate, 1.12 equivalents of Na-acetate as base, 10 ml DMA, yield: determination by GC analysis with diethyleneglycol-dibutylether as internal standard.

[a] TON in units of mol converted substrate per mol catalyst.

[b] TOF = TON h^{-1}.

acetate as base. No additives were required for a fast and selective reaction to give the coupling product (*E*)-4-acetylcinnamate. It is interesting to note that there is no induction period in this catalytic reaction.

With complex **3**, a turnover frequency (TOF) of 29 000 mol product per mol catalyst per hour and turnover numbers of more than 400 000 mol product per mol catalyst could be achieved in reactions which were not optimized (Table 1, entry 5). Decreasing the reaction temperature from 120 to 100 °C (Table 1, entry 3) does not lower the turnover number significantly. However, at room temperature the complexes are catalytically inactive. Furthermore, the formation of catalytically inactive palladium black was not observed when the catalysis was carried out between 100 and 120 °C even at long reaction times. Experiments with the precatalysts **3** and **4** (entries 3 and 6, Table 1) show that after all the substrates are consumed, more coupling can be observed when adding additional 3.5 mmol substrates to the reaction mixture. This increases the TON given in Table 1 (entry 3: 7800 mol product per mol catalyst; entry 6: 3900 mol product per mol catalyst) and leads to
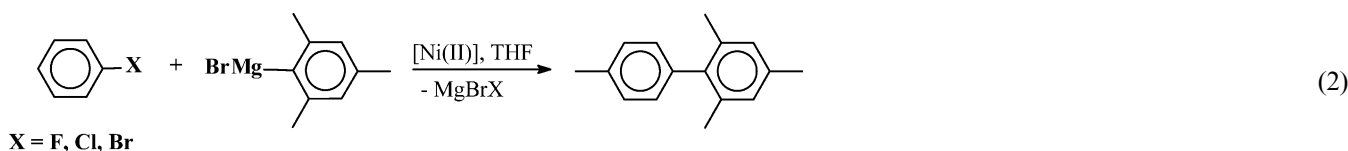
the conclusion that no decomposition of the active catalyst takes place.

In comparison with **1** and **2**, the catalysts **3** and **4** are much more active. When using either complex **3** or **4** as precatalyst in the Heck reaction, the aryl bromide is coupled quantitatively in 1 h, whereas **1** and **2** require 10 h for the total conversion (Table 1, entries 1–3 and 6). This is somewhat surprising, since no activating or

stabilizing ligands are involved in the catalytic cycle of the homoleptic, σ-organometallic Pd(II) compounds **3** and **4**.

It is known that Pd(OAc)$_2$ also shows high TON (560 000 mol product per mol Pd) when used as precatalyst in the Heck coupling between styrene and 4-bromoacetophenone [19b]. It could be possible that the catalytically active species formed from Pd(OAc)$_2$ has a structure similar to the active species generated by our homoleptic Pd(II) compounds **3** and **4**.

It is noteworthy that aryl chlorides were not activated with these catalysts.

2.4. Catalytic Kumada cross-coupling

The Ni complexes **5** and [(THF)$_4$Li$_4$(Me$_8$)Ni$_2$] (**6**) were surprisingly active in the catalytic Kumada cross-coupling [28–33]. In contrast, the palladium complexes **1**–**4** were catalytically inactive in this reaction. Table 2 lists some selected results of the reaction between MesitylMgBr and 4-methyl-aryl halides to form the mixed substituted biaryl (Eq. (2)):

X = F, Cl, Br   (2)

It is noteworthy that not only the organic bromide (Table 2, entries 1–5) can be used in this reaction, but also the chloride is active (Table 2, entries 6–10). In both cases, an induction period was not observed; however, longer reaction times are required in the reaction with the chloride, resulting in a maximum TON of 120 upon 1 h (Table 2, entry 7), whereas the organic bromide reacted three times faster (TON = 360,

Table 2
The Ni(II)-catalyzed Kumada cross-coupling with catalysts **5** and **6**

Entry	Complex	Halogene X	Temperature (°C)	Time (h)	Catalyst (mol%)	Conversion (%)[a]	TON[b]	TON mes–tol[c]	TON tol–tol[d]	TON (other products)
1	6	Br	20	1	0.2	72	360	337	17	6
2	6	Br	20	3	0.2	90	450	415	20	15
3	6	Br	20	4	0.2	92	470	425	23	22
4	5	Br	20	3	0.2	45	225	218	7	0
5	5	Br	20	24	0.2	92	460	450	10	0
6	6	Cl	20	24	1.5	95	63	31	24	8
7	6	Cl	20	1	0.2	24	120	75	20	25
8	6	Cl	20	8	0.2	50	250	143	52	55
9	6	Cl	20	96	0.2	90	450	228	132	90
10	5	Cl	20	24	2.0	>99	50	28	11	11
11	6	F	20	26.5	2.5	88	35	14	17	4
12	6	F	0	26.5	2.5	95	38	22	14	2
13	6	F	−25	26.5	2.5	54	22	11	10	1

Conditions: one equivalent of 4-tolyl halide (halides: X = Br, Cl, F), one equivalent of MesitylMgBr, solvents, THF.
[a] Amount of converted substrate 4-tolyl halide.
[b] In units of mol substrate per mol catalyst.
[c] Mol mesityl-4-tolyl/mol catalyst.
[d] Mol 4,4′-dimethylphenyl per mol catalyst; the yield was determined by GC analysis with n-decane as internal standard.

Table 2, entry 1) in a much more selective reaction. Furthermore, it is noteworthy that even the stable C–F bond of organic fluorides could be activated by using **6** as catalyst (Table 2, entries 11–13); however, the selectivity and the rate of this catalytic reaction were found to be relatively low.

Compared with a new (carbene)Ni catalyst, recently described by Herrmann et al. [34] to be active in the cross-coupling of organic fluorides, compound **6** reacted with a similar activity; however, the selectivity was lower. In this case, the most selective reaction was found at 0 °C (Table 2, entry 12). In a side reaction, the product of the homocoupling 4,4′-dimethyl-diphenyl (tol–tol) was observed. At 20 °C also the terphenylene derivative was formed, indicating an additional radical process at this temperature [35].

Table 2 does not represent the maximum TON for optimized catalytic reactions. Adding more of the substrates to the reaction mixture leads to more coupling product after the original amount of substrates is entirely converted by the active catalyst (Table 2). This means that the catalyst is still active. For example, the given TON for compound **6** can be increased to 690 mol converted substrate per mol catalyst by adding more 4-bromotoluene and MesitylMgBr to the reaction mixture (entry 3, Table 2).

5 is generally less active than **6**, but reaches higher selectivities (Table 2, entries 4, 5 and 10). Catalysts **5** and **6** are of interest for several reasons. According to the generally accepted mechanism of this catalytic reaction [28–33], the reductive elimination of the mixed biaryl is an essential step closing the catalytic cycle and resulting in the formation of low-valent nickel. Therefore, for stabilizing the Ni(0) the addition of neutral ligands such as phosphines or carbene-type ligands are required. In case of the complexes **5** and **6**, the presence of such a ligand is no prerequisite for the long-living catalysts.

In order to get a deeper insight into the starting steps of the catalytic cycle, the relatively slow reaction between MesitylMgBr and 4-methyl-phenyl chloride, using 1.5 mol% of complex **6** as precatalyst, was monitored by GC (Table 3).

In the first period (Table 3, entries 1–3), three reactions could be observed: the methyl transfer reaction from compound **6** to the mesityl group of MesMgBr to form 1,2,3,5-tetramethylbenzene, the cross-coupling re-action, and the formation of products of the homocou-pling (4,4′-dimethyl-diphenyl (tol–tol)). Furthermore, small amounts of terphenylenes were yielded. After about three of the four methyl groups at each Ni(II) center were transferred to mesityl groups, this methyl transfer stopped, whereas the catalyst was still active in both the cross-coupling reaction and in the homocou-pling reaction (Table 3, entries 4–6).

Additional stoichiometric experiments show that the coupling between the methyl groups of complex **6** and 4-

Table 3
Product distribution of the reaction between 4-chlorotoluene and MesitylMgBr in the presence of **6** as catalyst

Entry	Time (min)	Conversion (%) [a]	TON [b] mes–tol [c]	TON [b] tol–tol [c]	TON [b] terphenylene	TON [d] tetramethylbenzene	Methyl groups (%) [e]
1	10	32	13	6	2	4.3	60
2	30	45	17	9	4	4.9	68
3	90	56	20	12	5	5.6	78
4	210	69	24	15	6	5.7	80
5	390	81	28	19	7	5.7	80
6	1440	96	31	24	9	5.7	80

Conditions: 0.17 mmol **6**, 11.3 mmol = one equivalent of 4-tolyl chloride, one equivalent of MesitylMgBr, 29 ml THF.

[a] Amount of converted substrate 4-tolyl chloride.
[b] In units of mol converted 4-tolyl chloride per mol catalyst.
[c] mes–tol = mesityl-4-tolyl; tol–tol = 4,4′-dimethylphenyl.
[d] In units of mol converted MesitylMgBr per mol catalyst.
[e] Mol transferred methyl groups (tetramethylbenzene and p-xylene) per mol **6**; the yield was determined by GC analysis with n-decane as internal standard.

chlorotoluene in the absence of MesitylMgBr is a very slow and subordinate reaction, yielding no coupling products after 2 h. This corresponds with the above-mentioned results of the catalysis (Table 3, entry 6), where almost no p-xylene is formed (0.5%; 4% of the transferred methyl groups).

When using the phenyl complex **5** as catalyst in the cross-coupling reaction of 4-chlorotoluene and MesitylMgBr (Table 2, entry 10), also three of the four organyl groups (76%) were removed from the Ni(II) center during the catalytic cycle, analogous to complex **6**. However, the pathway was found to be very different from the above-mentioned reaction with **6**. 43% of the phenyl groups in **5** formed biphenyl (possibly formed by reductive elimination of two phenyl groups from the NiPh₄ fragment) and 33% of the phenyl groups in **5** yielded 4-methyl-biphenyl as a result of the coupling between Ni–Ph groups and 4-chlorotoluene.

In conclusion, both precatalysts **5** and **6** reacted in the catalytic cycle under elimination of three organyl groups from the metal. Therefore, we assume that in both cases the species [Ni–R] (R = CH₃, Ph) play an essential role in the catalytic cycle.

3. Experimental

3.1. General procedures

All manipulations were carried out by using modified Schlenk techniques under an atmosphere of argon. Prior to use, THF, diethyl ether, pentane and toluene were dried over potassium hydroxide and distilled over sodium/benzophenone. Methyllithium (1.6 M solution in diethyl ether, Fluka), phenyllithium (1.8 M solution in cyclohexane/diethyl ether, 70:30, Fluka), n-butyl-lithium (1.6 M solution in hexane, Aldrich), Mesitylthium (1.0 M solution in THF, Aldrich), 2-(2-aminoethyl)-pyridine (Fluka), 4-bromotoluene, 4-bro-

moacetophenone (Aldrich) were used as received; 4-chlorotoluene, 4-fluorotoluene, n-decane and diethyle-neglycol-dibutylether (Aldrich) were distilled and dried over molecular sieve, and n-butyl acrylate (Aldrich) was dried over molecular sieve. ¹H- and ¹³C-NMR spectra were recorded on a Bruker Avance 200 and on a Bruker Avance 400 spectrometer. Mass spectra were recorded on a Finnigan MAT SSQ 710. Values for m/z are for the most intense peak of isotope envelope. The measured isotopic patterns for the palladium-containing species are in good agreement with the calculated isotopic patterns using the program ICIS (version 8.2.1, Finnigan). Elemental analyses were performed with a Leco CHNS-932 and an Elementar Vario EL III. Ni analyses were obtained by titration of a solution in dilute hydrochloric acid with 0.01 M EDTA using murexid as indicator. Li and Pd analyses were performed by ETV-ICP-MS (Perkin–Elmer Elan 6000, Perkin–Elmer HGA 500).

The ligands N,N'-bis(2-pyridylethyl)-1,2-bis-(2,4,6-trimethylphenyl-imino)-ethane-1,2-diamine (H₂Y) and N,N'-bis(diphenylphosphino-3-propyl)-1,2-bis-(2,4,6-trimethylphenyl-imino)-ethane-1,2-diamine (H₂Z) were prepared according to the described methods [12,13]; [(THF)₄Li₄(Me₈)Ni₂] (**6**) was prepared as described recently [8]; (COD)Pd(CH₃)Cl was obtained following the procedure described in [36].

3.2. Crystal structure determination

The intensity data for the compounds were collected on a Nonius KappaCCD diffractometer, using graphite-monochromated Mo–K$_\alpha$ radiation. Data were corrected for Lorentz and polarization effects, but not for absorption effects [37,38].

The structures were solved by direct methods (SHELXS [39]) and refined by full-matrix least-squares techniques against Fo2 (SHELXL-97 [40]). All hydrogen atoms were included at calculated positions with fixed thermal

parameters. All non-hydrogen atoms were refined anisotropically [40]. XP (SIEMENS Analytical X-ray Instruments, Inc.) was used for structure representations.

3.2.1. Crystal data for 1

$C_{36}H_{44}N_6Pd_2 \cdot 1.25C_4H_8O$, $Mr = 863.70$ g mol^{-1}, colorless prism, size $0.12 \times 0.12 \times 0.08$ mm^3, orthorhombic, space group $Pbcn$, $a = 23.7807(9)$ Å, $b = 15.0256(6)$ Å, $c = 23.6595(7)$ Å, $V = 8454.0(5)$ Å^3, $T = -90$ °C, $Z = 8$, $\rho_{calcd} = 1.36$ g cm^{-3}, $\mu(\text{Mo–K}_\alpha) = 8.88$ cm^{-1}, $F(0\,0\,0) = 3552$, 17 940 reflections in h ($-30/30$), k ($-19/19$), l ($-30/30$), measured in the range $1.60° \leq \Theta \leq 27.46°$, completeness $\Theta_{max} = 99.2\%$, 9609 independent reflections, $R_{int} = 0.061$, 3854 reflections with $F_o > 4\sigma(F_o)$, 451 parameters, five restraints, $R_{1_{obs}} = 0.052$, $wR_{2_{obs}} = 0.145$, $R_{1_{all}} = 0.134$, $wR_{2_{all}} = 0.162$, GOOF = 0.944, largest difference peak and hole: $0.977/-0.563$ e Å^{-3}.

3.2.2. Crystal data for 2

$C_{70}H_{78}N_4P_2Pd_2$, $Mr = 1250.10$ g mol^{-1}, colorless prism, size $0.22 \times 0.20 \times 0.10$ mm^3, monoclinic, space group $C2/c$, $a = 37.920(1)$ Å, $b = 12.6793(4)$ Å, $c = 13.6274(5)$ Å, $\beta = 110.546(2)°$, $V = 6135.3(3)$ Å^3, $T = -90$ °C, $Z = 4$, $\rho_{calcd} = 1.353$ g cm^{-3}, $\mu(\text{Mo–K}_\alpha) = 6.83$ cm^{-1}, $F(0\,0\,0) = 2592$, 11 623 reflections in h ($-44/47$), k ($-15/16$), l ($-17/17$), measured in the range $2.35° \leq \Theta \leq 27.47°$, completeness $\Theta_{max} = 99.2\%$, 6961 independent reflections, $R_{int} = 0.032$, 4879 reflections with $F_o > 4\sigma(F_o)$, 352 parameters, 0 restraints, $R_{1_{obs}} = 0.033$, $wR_{2_{obs}} = 0.072$, $R_{1_{all}} = 0.052$, $wR_{2_{all}} = 0.075$, GOOF = 0.943, largest difference peak and hole: $0.494/-0.592$ e Å^{-3}.

3.2.3. Crystal data for 3

$C_{24}H_{56}Li_4O_4Pd_2$, $Mr = 649.25$ g mol^{-1}, colorless prism, size $0.10 \times 0.09 \times 0.04$ mm^3, monoclinic, space group $P2_1/c$, $a = 10.5969(2)$ Å, $b = 26.1649(4)$ Å, $c = 12.1083(3)$ Å, $\beta = 115.8340(1)°$, $V = 3021.71(10)$ Å^3, $T = -90$ °C, $Z = 4$, $\rho_{calcd} = 1.427$ g cm^{-3}, $\mu(\text{Mo–K}_\alpha) = 12.14$ cm^{-1}, $F(0\,0\,0) = 1344$, 12 268 reflections in h ($-13/13$), k ($-33/27$), l ($-15/15$), measured in the range $1.56° \leq \Theta \leq 27.46°$, completeness $\Theta_{max} = 99.2\%$, 6863 independent reflections, $R_{int} = 0.023$, 5426 reflections with $F_o > 4\sigma(F_o)$, 307 parameters, 0 restraints, $R_{1_{obs}} = 0.035$, $wR_{2_{obs}} = 0.089$, $R_{1_{all}} = 0.049$, $wR_{2_{all}} = 0.096$, GOOF = 1.022, largest difference peak and hole: $0.525/-0.613$ e Å^{-3}.

3.2.4. Crystal data for 4

$C_{40}H_{52}Li_2O_4Pd$, $Mr = 717.10$ g mol^{-1}, colorless prism, size $0.10 \times 0.09 \times 0.05$ mm^3, triclinic, space group $P\bar{1}$, $a = 9.0853(4)$ Å, $b = 11.5980(5)$ Å, $c = 17.2638(8)$ Å, $\alpha = 92.371(3)°$, $\beta = 94.538(3)°$, $\gamma = 98.325(3)°$, $V = 1791.7(1)$ Å^3, $T = -90$ °C, $Z = 2$, $\rho_{calcd} = 1.329$ g

cm^{-3}, $\mu(\text{Mo–K}_\alpha) = 5.57$ cm^{-1}, $F(0\,0\,0) = 752$, 13 042 reflections in h ($-11/11$), k ($-15/15$), l ($-19/22$), measured in the range $4.10° \leq \Theta \leq 27.45°$, completeness $\Theta_{max} = 98.4\%$, 8071 independent reflections, $R_{int} = 0.059$, 6166 reflections with $F_o > 4\sigma(F_o)$, 424 parameters, 0 restraints, $R_{1_{obs}} = 0.065$, $wR_{2_{obs}} = 0.155$, $R_{1_{all}} = 0.093$, $wR_{2_{all}} = 0.174$, GOOF = 1.120, largest difference peak and hole: $1.818/-1.433$ e Å^{-3}.

3.2.5. Crystal data for 5

$C_{40}H_{52}Li_2NiO_4$, $Mr = 669.40$ g mol^{-1}, colorless prism, size $0.20 \times 0.18 \times 0.12$ mm^3, triclinic, space group $P\bar{1}$, $a = 9.0874(5)$ Å, $b = 11.5830(6)$ Å, $c = 17.2180(8)$ Å, $\alpha = 90.648(3)°$, $\beta = 95.572(3)°$, $\gamma = 99.042(3)°$, $V = 1780.73(16)$ Å^3, $T = -90$ °C, $Z = 2$, $\rho_{calcd} = 1.248$ g cm^{-3}, $\mu(\text{Mo–K}_\alpha) = 5.84$ cm^{-1}, $F(0\,0\,0) = 716$, 12 229 reflections in h ($-11/11$), k ($-14/15$), l ($-22/22$), measured in the range $1.19° \leq \Theta \leq 27.48°$, completeness $\Theta_{max} = 98.8\%$, 8049 independent reflections, $R_{int} = 0.051$, 5495 reflections with $F_o > 4\sigma(F_o)$, 503 parameters, 0 restraints, $R_{1_{obs}} = 0.088$, $wR_{2_{obs}} = 0.119$, $R_{1_{all}} = 0.145$, $wR_{2_{all}} = 0.134$, GOOF = 1.056, largest difference peak and hole: $0.434/-0.488$ e Å^{-3}.

3.3. Complex 1

A solution of H_2Y (0.588 g, 1.11 mmol) in THF (40 ml) was stirred at -78 °C. n-Butyllithium, dissolved in hexane (1.25 ml, 2.0 mmol), was added dropwise. After stirring the solution at room temperature for 30 min and cooling down to -78 °C, a solution of $(COD)Pd(CH_3)Cl$ (0.530 g, 2.00 mmol) in THF (30 ml) was added. The solution was stirred for 18 h and allowed to warm to room temperature. After removing the solvents by oil pump vacuum, the obtained solid was extracted with toluene (60 ml). The extract was filtered and the residue was washed with toluene (10 ml). The unified clear solution was concentrated by oil pump vacuum to dryness and was diluted with diethyl ether (10 ml). The precipitate was filtered, washed with diethyl ether (20 ml) and dried by oil pump vacuum (4 h) at room temperature. Yield: 0.508 g (55%) of the desired product containing 0.8 equivalents of diethyl ether. Complex 1 without non-coordinated solvent was obtained by recrystallization from toluene in lower yields. Single crystals suitable for X-ray determination were isolated from THF-d_8 at room temperature. Anal. Calcd. for $C_{36}H_{44}N_6Pd_2$: C, 55.89; H, 5.73; N, 10.86. Found: C, 54.23; H, 5.82; N, 10.07%. MS (DEI) m/z: 757 $[M-CH_3]^+$ (0.6%), 742 $[M-2CH_3]^+$ (0.2%), 636 $[M-2CH_3-Pd]^+$ (0.2%), 530 $[M-2CH_3-2Pd]^+$ (1.7%). ^{1}H-NMR (200 MHz, THF-d_8): δ -0.55 (s, 6H, CH_3, $Pd-CH_3$), 2.18 (s, 12H, CH_3, mes ortho), 2.29 (s, 6H, CH_3, mes para), 2.26 (m, 4H, CH_2), 2.86 (m, 4H, CH_2), 6.65 (s, 4H, mes meta), 7.09–7.18 (m, 4H, 3-, 5-pyridyl), 7.68 (t ($^3J_{HH} = 7.6$ Hz), 2H, CH, 4-pyridyl), 8.35 (d

($^3J_{HH}$ = 5.7 Hz), 2H, CH, *6-pyridyl*) ppm. ^{13}C-NMR (50 MHz, THF-d_8): δ 4.9 (CH$_3$, Pd–CH$_3$), 19.4 (CH$_3$, *mes para*), 21.0 (CH$_3$, *mes ortho*), 43.4 (CH$_2$), 44.6 (CH$_2$), 123.1 (CH, *5-pyridyl*), 125.4 (CH, *3-pyridyl*), 127.7 (CH, *mes meta*), 132.1 (C), 138.0 (CH, *4-pyridyl*), 146.8 (C), 152.4 (CH, *6-pyridyl*), 162.2, 167.3 (C) ppm.

3.4. Complex 2

The compound was prepared as a light yellow solid, analogous to **1** using H$_2$Z (0.882 g, 1.14 mmol). Yield: 0.400 g (33%) of **2** containing one equivalent of non-coordinated THF. Single crystals of **2** which contain three molecules of non-coordinated benzene-d_6 per dimeric unit suitable for an X-ray analysis were grown from benzene-d_6 at room temperature. Anal. Calcd. for C$_{52}$H$_{60}$N$_4$P$_2$Pd$_2$·C$_4$H$_8$O: C, 61.82; H, 6,30; N, 5.15. Found: C, 60.71; H, 6.29; N, 4.90%. MS (DEI): *m/z*: 999 [M–CH$_3$]$^+$ (3%), 693 [M–2CH$_3$–Pd–PPh$_2$]$^+$ (0.5%). ^{1}H-NMR (400 MHz, THF-d_8): δ –0.85 (d ($^3J_{HP}$ = 3.2 Hz), 6H, CH$_3$, Pd–CH$_3$), 1.44–1.51 (m, 4H, CH$_2$), 1.84–1.90 (m, 4H, CH$_2$), 2.15 (s, 6H, CH$_3$, *mes para*), 2.31 (s, 12H, CH$_3$, *mes ortho*), 2.59–2.61 (m, 4H, CH$_2$), 6.67 (s, 4H, CH, *mes meta*), 7.37–7.38 (m, 12H, CH, *Ph*), 7.65–7.69 (m, 8H, CH, *Ph*) ppm. ^{13}C-NMR (100 MHz, THF-d_8): δ 2.3 (d ($^2J_{CP}$ = 13 Hz), CH$_3$, Pd–CH$_3$), 19.8 (CH$_3$, *mes ortho*), 20.9 (CH$_3$, *mes para*), 27.3 (d ($^1J_{CP}$ = 27 Hz, CH$_2$)), 28.3 (d ($^2J_{CP}$ = 8 Hz, CH$_2$)), 51.9 (CH$_2$), 127.8 (CH, *mes meta*), 128.8–128.9, 130.6–130.7 (CH), 131.2, 133.1 (C), 134.1–134.3 (CH), 134.5, 134.9, 146.3, 169.7 (C) ppm. ^{31}P-NMR (162 MHz, THF-d_8): δ 36.7 ppm.

3.5. Complex 3

A solution of **1** (0.155 g, 0.20 mmol) in THF (40 ml) was stirred at –78 °C. Methyllithium, dissolved in diethyl ether (0.9 ml, 1.44 mmol), was added dropwise. The solution was stirred for 18 h and allowed to warm to room temperature. The reaction mixture was filtered and the clear solution was concentrated in oil pump vacuum to 5 ml. Colorless crystals were formed at –25 °C after 48 h. The solvent was removed and the solid was washed with toluene (10 ml) and pentane (10 ml). It was dried by overflowing argon for 5 min. A pyrophoric colorless powder was obtained. Yield: ca. 20%. Single crystals of **3** suitable for X-ray determination were grown from THF at –18 °C. Anal. Calcd. for C$_{24}$H$_{56}$O$_4$Li$_4$Pd$_2$: Li, 4.28. Found: Li, 4.63% (ETV-ICP-MS); ^{1}H-NMR (400 MHz, benzene-d_6): δ –0.11 (s, 24H, CH$_3$), 1.30 (m, 16H, CH$_2$), 3.72 (m, 16H, CH$_2$) ppm. ^{13}C-NMR (100 MHz, benzene-d_6): δ –7.6 (s, CH$_3$), 25.5 (s, CH$_2$), 68.7 (s, CH$_2$) ppm. ^{7}Li-NMR (156 MHz, benzene-d_6): δ 9.3 ppm.

3.6. Complex 4

The compound was prepared as a colorless micro-crystalline solid, using [(acac)Pd(oxam)Pd(acac)] (0.547 g, 0.64 mmol) in THF (80 ml) and eight equivalents of phenyllithium, dissolved in cyclohexane/diethyl ether (70:30) (2.9 ml, 5.2 mmol). Yield: 220 mg (24%). Single crystals of **4** suitable for X-ray determination were obtained from THF at –25 °C. The crystals contain four THF molecules per Pd unit. Anal. Calcd. for C$_{40}$H$_{52}$O$_4$Li$_2$Pd: Li, 1.94; Pd, 14.84. Found: Li, 2.16 (ETV-ICP-MS), Pd, 14.55% (ETV-ICP-MS). ^{1}H-NMR (400 MHz, benzene-d_6): δ 1.38 (m, 16H, CH$_2$), 3.51 (m, 16H, CH$_2$), 6.95–6.99 (m, 1H, CH), 7.11–7.22 (m, 13H, CH), 7.44–7.47 (m, 4H, CH), 8.16 (d, 2H, CH) ppm. ^{13}C-NMR (100 MHz, benzene-d_6): δ 25.9 (s, CH$_2$), 68.0 (s, CH$_2$), 122.2 (s, CH), 126.7–129.2 (m, C, CH), 141.2 (s, CH) ppm. ^{7}Li-NMR (156 MHz, benzene-d_6): δ 7.1 ppm.

3.7. Complex 5

The compound was prepared as a light yellow microcrystalline solid, analogous to **4** using [(acac)Ni(oxam)Ni(acac)] (0.758 g, 0.86 mmol) in THF (80 ml) and eight equivalents of phenyllithium, dissolved in cyclohexane/diethyl ether (70:30) (3.8 ml, 6.88 mmol). Yield: 250 mg (22%). Single crystals of **5** suitable for X-ray determination were obtained from THF at –18 °C. The crystals contain four THF molecules per Ni unit. Anal. Calcd. for C$_{40}$H$_{52}$O$_4$Li$_2$Ni: Li, 2.07; Ni, 8.77. Found: Li, 2.17 (ETV-ICP-MS); Ni, 8.75% (ETV-ICP-MS), 9.08% (titration). ^{1}H-NMR (200 MHz, benzene-d_6): δ 1.36 (m, 16H, CH$_2$), 3.41 (m, 16H, CH$_2$), 6.84–7.18 (m, 14H, CH), 7.46–7.50 (m, 2H, CH), 8.28–8.31 (m, 4H, CH) ppm. ^{13}C-NMR (50 MHz, benzene-d_6): δ 25.7 (s, CH$_2$), 67.8 (s, CH$_2$), 127.5–129.0 (m, C, CH) ppm. ^{7}Li-NMR (156 MHz, benzene-d_6): δ 6.5 ppm.

3.8. Heck reaction

0.050 mmol of the catalyst were dissolved in 20 ml dry THF containing 0.1 ml of a 1.6-M solution of methyllithium. In a typical experiment, 6.25 mmol (1.244 g) 4-bromoacetophenone and 7 mmol (0.547 g) anhydrous sodium acetate as base were placed in a 25-ml two-necked flask equipped with stirring bar, reflux condenser and septum. The flask was degassed under vacuum and purged with argon to ensure an inert reaction atmosphere. Through the septum were added 10 ml of *N*,*N*-dimethylacetamide as solvent, 0.5 g of diethylene-glycol-dibutylether as GC standard and 6.75 mmol *n*-butyl acrylate. The reaction mixture was thoroughly stirred and heated to the appropriate reaction temperature at which it was held for 5 min. Either 0.5 ml of the catalyst solution for complexes **1**–**3** (1.25 µmol) or 1 ml

(2.5 µmol) of the catalyst solution for complex **4** was added. Samples of 0.5 ml were taken after the appropriate time intervals, hydrolyzed with 2 ml distilled water and extracted with 2 ml CH_2Cl_2. The organic phase was dried over K_2CO_3 and stored at $-25\,^\circ$C until GC analysis for the determination of yield and turnover number could be performed.

3.9. Kumada cross-coupling reaction

For each catalytic reaction, a defined amount of either complex **5** or **6** was weighed into a small glass tube under an argon atmosphere and sealed by fusing the open end, because of the extreme sensitivity of complexes **5** and **6** towards air and moisture no standard catalyst solution was prepared. Together with one equivalent of the 4-methyl-benzyl halide, the sealed catalyst was placed into a Schlenk tube and purged with argon. One equivalent of a 1.0-M solution of MesitylMgBr in THF, THF as solvent and 0.8 g *n*-decane as internal GC standard were added to the reaction mixture through a septum. The same concentration of substrates was ensured for every amount of weighed in catalyst (Table 2: entries 1–3 and 7–9: 7.8 µmol **6**, 3.9 mmol substrates, 10 ml THF; entries 4–5: 10.9 µmol **5**, 5.5 mmol substrates, 14 ml THF; entry 6: 0.17 mmol **6**, 11.3 mmol substrates, 29 ml THF; entry 10: 0.06 mmol **5**, 3.0 mmol substrates, 7.7 ml THF; entry 11: 0.08 mmol **6**, 3.4 mmol substrates, 8.7 ml THF; entries 12–13: 0.06 mmol **6**, 2.3 mmol substrates, 6.0 ml THF). If necessary, the mixture was cooled to the appropriate temperature; otherwise, it was held at room temperature. The reaction started by breaking the glass tube and dissolving the catalyst. Samples of 0.5 ml were taken after certain time intervals, hydrolyzed with half concentrated hydrochloric acid (1.0 ml) and extracted with toluene (1.0 ml). The organic phase was dried over K_2CO_3 and transferred into vials. The yield determination was done by gas chromatography.

4. Supplementary material

Crystallographic data for the structural analysis have been deposited with the Cambridge Crystallographic Data Centre, CCDC Nos. 202218–202222 for compounds **1**–**5**. Copies of this information may be obtained free of charge from The Director, CCDC, 12 Union Road, Cambridge, CB2 1EZ, UK (Fax: +44-1223-336033; e-mail: deposit@ccdc.cam.ac.uk or www: http://www.ccdc.cam.ac.uk).

References

[1] E. Kurras, J. Otto, J. Organomet. Chem. 4 (1965) 114.
[2] J. Krause, G. Marx, G. Schödl, J. Organomet. Chem. 21 (1970) 159.
[3] S. Hao, S. Gambarotta, C. Bensimon, J. Am. Chem. Soc. 114 (1992) 3556.
[4] S. Hao, J.-I. Song, P. Berno, S. Gambarotta, Organometallics 13 (1994) 1326.
[5] F.A. Cotton, J.M. Troup, D.H. Webb, G. Williamson, J. Wilkinson, J. Am. Chem. Soc. 96 (1974) 3824.
[6] F.A. Cotton, L.D. Gage, L.W. Mertis, G. Shive, J. Wilkinson, J. Am. Chem. Soc. 98 (1976) 6922.
[7] R. Wyrwa, H. Görls, Z. Anorg. Allg. Chem. 625 (1999) 1904.
[8] D. Walther, M. Stollenz, H. Görls, Organometallics 20 (2001) 4221.
[9] E. Ihara, T. Fujimura, H. Yasuda, T. Maruo, N. Kanehisa, Y. Kai, J. Polym. Sci. A38 (2000) 4764.
[10] R. Taube, G. Honymus, Angew. Chem. 87 (1975) 291.
[11] J.J.H. Edema, S. Gambarotta, F. van Bolhuis, W.J.J. Smeets, A.L. Spekk, M.Y. Chiang, J. Organomet. Chem. 389 (1990) 47.
[12] P. Langer, M. Döring, J. Wuckelt, H. Görls, Eur. J. Inorg. Chem. (2001) 805.
[13] D. Walther, M. Stollenz, L. Böttcher, H. Görls, Z. Anorg. Allg. Chem. 627 (2001) 1560.
[14] N. Theyssen, D. Walther, T. Döhler, H. Görls, Eur. J. Inorg. Chem. (2001) 2049.
[15] For a recent review see: (a) A.F. Littke, G.C. Fu, Angew. Chem. 114 (2002) 4351;
(b) A.F. Littke, G.C. Fu, Angew. Chem Int. Ed. 41 (2002) 4176 (and references therein).
[16] (a) A. de Meijere, F. Meyer, Angew. Chem. 106 (1994) 2473;
(b) A. de Meijere, F. Meyer, Angew. Chem Int. Ed. 33 (1994) 2379.
[17] V.V. Grushin, H. Alper, Chem. Rev. 106 (1994) 2473.
[18] W. Cabri, I. Caudiani, Acc. Chem. Res. 28 (1995) 2.
[19] (a) W.A. Herrmann, C. Broßmer, K. Öfele, C.-P. Reisinger, T. Riermeier, M. Beller, H. Fischer, Angew. Chem. 107 (1995) 1989;
(b) W.A. Herrmann, C. Broßmer, K. Öfele, C.-P. Reisinger, T. Riermeier, M. Beller, H. Fischer, Angew. Chem. Int. Ed. 28 (1995) 1844;
(c) W.A. Herrmann, C. Broßmer, C.-P. Reisinger, T. Riermeier, K. Öfele, M. Beller, Chem. Eur. J. 3 (1997) 1357.
[20] W.A. Herrmann, V. Böhm, J. Organomet. Chem. 572 (1999) 141.
[21] W.A. Herrmann, V. Böhm, C.-P. Reisinger, J. Organomet. Chem. 576 (1999) 23.
[22] (a) W.A. Herrmann, M. Elison, J. Fischer, C. Köcher, G.R.J. Artus, Angew. Chem. 107 (1995) 2602;
(b) W.A. Herrmann, M. Elison, J. Fischer, C. Köcher, G.R.J. Artus, Angew. Chem. Int. Ed. 34 (1995) 2371;
(c) W.A. Herrmann, C.-P. Reisinger, M.J. Spiegler, J. Organomet. Chem. 557 (1998) 93.
[23] W.A. Herrmann, Th. Weskamp, V.P.W. Böhm, J. Organomet. Chem. 585 (1999) 348.
[24] W.A. Herrmann, V. Böhm, Chem. Eur. J. 6 (2000) 1017.
[25] D.S. McGuiness, K.J. Cavell, Organometallics 19 (2000) 741.
[26] M. Beller, A. Zapf, Synlett (1998) 792.

[27] A. Zapf, M. Beller, Chem. Eur. J. 7 (2001) 2908.

[28] E. Negishi, F. Liu, in: F. Diederich, P.J. Stang (Eds.), Metal-catalyzed Cross-coupling Reactions, Wiley-VCH, New York, 1998, p. 34 (and references therein).

[29] (a) D.J. Cárdenas, Angew. Chem. 111 (1999) 3201;
(b) D.J. Cárdenas, Angew. Chem. Int. Ed. Engl. 38 (1999) 3018.

[30] E. Negishi, T. Takahashi, S. Baba, D.E. van Horn, N. Okukado, J. Am. Chem. Soc. 109 (1987) 2393.

[31] E. Negishi, E.T. Takahashi, K. Akiyoshi, J. Organomet. Chem. 334 (1987) 181.

[32] C. Amatore, M. Azzabi, A. Jutand, J. Am. Chem. Soc. 113 (1991) 8375.

[33] J.F. Hartwig, F. Paul, J. Am. Chem. Soc. 117 (1995) 5373.

[34] W.A. Herrmann, V.P.W. Böhm, C.W.K. Gstöttmayr, T. Weskamp, Angew. Chem. 18 (2001) 3500.

[35] G. Smith, J.K. Kochi, J. Organomet. Chem. 198 (1980) 199.

[36] R.E. Rülke, J.M. Ernsting, A.L. Spek, C.J. Elsevier, P.W.N.M. van Leeuwen, K. Vrieze, Inorg. Chem. 32 (1993) 5769.

[37] COLLECT, Data Collection Software, Nonius B.V., Netherlands, 1998.

[38] Z. Otwinowski, W. Minor, Processing of X-ray diffraction data collected in oscillation mode, in: C.W. Carter, R.M. Sweet (Eds.), Methods in Enzymology, Vol. 276, Macromolecular Crystallography, Part A, Academic Press, New York, 1997, pp. 307–326.

[39] G.M. Sheldrick, Acta Crystallogr. Sect. A 46 (1990) 467.

[40] G.M. Sheldrick, SHELXL-97 (Release 97-2), University of Göttingen, Göttingen, Germany, 1997.